The influence of time, shape and tides on the obliquity of Mercury

Benoît Noyelles & Christoph Lhotka

University of Namur, Dpt of Mathematics and Namur Center for Complex Systems (NAXYS), 8 Rempart de la Vierge, B-5000 Namur, Belgium, tel: +3281724940 fax: +3281724914

benoit.noyelles,clhotka@fundp.ac.be

ABSTRACT

Earth-based radar observations of the rotational dynamics of Mercury (Margot et al. 2012) combined with the determination of its gravity field by MESSENGER (Smith et al. 2012) give clues on the internal structure of Mercury, in particular its polar moment of inertia C, deduced from the obliquity (2.04 ± 0.08) arcmin.

The dynamics of the obliquity of Mercury is a very-long term motion (a few hundreds of kyrs), based on the regressional motion of Mercury's orbital ascending node. This paper, following the study of Noyelles & D'Hoedt (2012), aims at first giving initial conditions at any time and for any values of the internal structure parameters for numerical simulations, and at using them to estimate the influence of usually neglected parameters on the obliquity, like J_3, the Love number k_2 and the secular variations of the orbital elements. We use for that averaged representations of the orbital and rotational motions of Mercury, suitable for long-term studies.

We find that J_3 should alter the obliquity by 250 milli-arcsec, the tides by 100 milli-arcsec, and the secular variations of the orbital elements by 10 milli-arcsec over 20 years. The resulting value of C could be at the most changed from $0.346mR^2$ to $0.345mR^2$

Subject headings: Mercury — Celestial Mechanics — Resonances, spin-orbit — Rotational dynamics

1. Introduction

The space missions MESSENGER (NASA) and BepiColombo (ESA / JAXA) (Balogh et al. 2007) are opportunities to have a better knowledge of Mercury, in particular its rotational

dynamics and its internal structure. The size of an outer molten core can be inverted from the well-known Peale experiment (Peale 1976; Peale et al. 2002) in measuring separately the obliquity of Mercury, yielding the polar momentum of inertia C, and the longitudinal librations, yielding the polar momentum of the mantle C_m. This last assertion is based on the assumption that the longitudinal librations of the mantle are decoupled from the other layers, what can be doubtful if Mercury has a significant inner core (Veasey & Dumberry 2011; Van Hoolst et al. 2012). But this does not affect the determination of C.

The determination of C from the obliquity is based on the assumptions that Mercury is at the Cassini State 1, and that it behaves as a rigid body over the timescales relevant for the variations of the obliquity, i.e. a few hundreds of years, due to the regressional motion of Mercury's orbital nodes. The Cassini State 1 is a dynamical equilibrium in which Mercury is in a 3:2 spin-orbit resonance (Pettengill & Dyce 1965; Colombo 1965), and the small free librations around the equilibrium have been damped with enough efficiency so that the obliquity of Mercury can be considered as an equilibrium obliquity. Peale (2005) estimated the damping timescale to be of the order of 10^5 years for the free librations and the free precession of the spin, in considering the tidal dissipation and the core-mantle friction. The presence of Mercury near the Cassini State 1, has been confirmed by Earth-based radar observations (Margot et al. 2007, 2012), giving an obliquity of 2.04 ± 0.08 arcminutes. The variations of the obliquity can be considered as small and adiabatic (Bills & Comstock 2005; Peale 2006; Bois & Rambaux 2007; D'Hoedt & Lemaitre 2008).

It is commonly accepted that the obliquity ϵ should be inverted using Peale's formula (Peale 1969), that reads as (Yseboodt & Margot 2006):

$$\epsilon = -\frac{C\dot{\Omega}\sin\iota}{C\dot{\Omega}\cos\iota + 2nmR^2\left(\frac{7}{2}e - \frac{123}{16}e^3\right)C_{22} - nmR^2\left(1-e^2\right)^{-3/2}C_{20}}, \tag{1}$$

where n is the orbital mean motion of Mercury, m its mass, R its mean radius, e its orbital eccentricity, $C_{20} = -J_2$ and C_{22} are the 2 most relevant coefficients of the gravity field of Mercury, and ι and $\dot{\Omega}$ are the inclination and nodal precession rate of the orbit of Mercury with respect to a Laplace Plane. The Laplace Plane is a reference plane, determined so as to minimize the variation of the inclination ι. In this way, ι and $\dot{\Omega}$ are assumed to be constant, and also ϵ as a consequence. There are several ways to define the Laplace Plane (Yseboodt & Margot 2006; Bois & Rambaux 2007; D'Hoedt et al. 2009), and so ι and $\dot{\Omega}$ depend on the chosen definition.

In order to bypass the uncertainty on the Laplace Plane, Noyelles & D'Hoedt (2012) proposed a Laplace Plane-free study of the obliquity, using averaged equations of the rotational motion, averaged variations of the eccentricity, inclination and the associated angles,

and a quasi-periodic representation of these quantities. This yields a quasi-periodic representation of the equilibrium obliquity that is very close to the Cassini State over the domain of validity of the JPL DE 406 ephemerides (Standish 1998), i.e. 6,000 years between JED 0625360.50 (-3000 February 23) to 2816912.50 (+3000 May 06). The inertial reference frame is the ecliptic at J2000. This approach allows to consider the small variations of the orbital elements.

The spacecraft MESSENGER currently orbiting around Mercury has recently given us accurate gravity coefficients (Tab.1) (Smith et al. 2012), this is the opportunity to refine our model of the obliquity and to consider usually neglected effects like the tides or higher order gravity coefficients.

Table 1: The gravity field coefficients of Mercury derived from MESSENGER data (Smith et al. 2012). These are unnormalized coefficients while Smith et al. give them normalized.

$C_{20} = -J_2$	$(-5.031 \pm 0.02) \times 10^{-5}$
C_{21}	$(-5.99 \pm 6.5) \times 10^{-8}$
S_{21}	$(1.74 \pm 6.5) \times 10^{-8}$
C_{22}	$(8.088 \pm 0.065) \times 10^{-6}$
S_{22}	$(3.22 \pm 6.5) \times 10^{-8}$
$C_{30} = -J_3$	$(-1.188 \pm 0.08) \times 10^{-5}$
$C_{40} = -J_4$	$(-1.95 \pm 0.24) \times 10^{-5}$

We first present how we average the equations ruling the rotational dynamics of Mercury (Sect.2). This averaging is more accurate than the one given in (Noyelles & D'Hoedt 2012), i.e. it is done to higher order in eccentricity. Then we explain how we derive 2 new formulae for the obliquity, one analytically (Sect.3), with an approach slightly different than Peale's, and one numerically (Sect.4). Then the reliability of these formulae are tested and additional effects are discussed (Sect.5). The influence on the interpretation of the internal structure of Mercury is finally addressed (Sect.6).

2. The dynamical model

The basic model behind the spin-orbit dynamics of the Sun-Mercury system is given in terms of the Hamiltonian:

$$H = H_K + H_T - (G_c M m) V_G, \tag{2}$$

where G_c is the gravitational constant, M is the mass of the Sun and $m \simeq 1.6 \cdot 10^{-7}[M]$ is the mass of Mercury. The symbol H_K labels the unperturbed Kepler problem:

$$H_K = -\frac{m^3 \mu^2}{2L_o^2} \ , \tag{3}$$

with the constant μ given by $\mu = G_c(M + m)$, and $L_o = m\sqrt{\mu a}$ is the orbital angular momentum, which depends on the semi-major axis of Mercury $a \simeq 0.387[AU]$. H_T defines the free rotational motion of Mercury:

$$H_R = \frac{1}{2}\left(G^2 - L^2\right)\left(\frac{\sin^2(l)}{A} + \frac{\cos^2(l)}{B}\right) + \frac{L^2}{2C} \ , \tag{4}$$

where $A \leq B < C$ are the principal moments of inertia, G is the norm of the angular momentum $\vec{G}$, $L = G\cos(J)$ is the projection of $\vec{G}$ onto the polar figure axis of Mercury, with the angle J usually called the wobble, and l is the conjugated angle to the action L.

2.1. General form of the potential

The gravitational interaction of the orbital and rotational dynamics is given by the potential V_G. It can be expanded into spherical harmonics, and takes the form, after (Cunningham 1970; Bertotti & Farinella 1990):

$$V_G = \sum_{n=0}^{\infty}\sum_{m=0}^{n} \frac{R^n}{r^{n+1}} P_{nm}(\sin\varphi)\left(C_{nm}\cos(m\lambda) + S_{nm}\sin(m\lambda)\right) \ , \tag{5}$$

where $R \simeq 2439.7[km]$ (Archinal et al. 2011) is the radius of Mercury, r is the distance of the center of mass of Mercury from the center of mass of the Sun, $P_{nm} = P_{nm}(u)$ are the associated Legendre polynomials, which are defined in terms of the standard Legendre polynomials $P_n = P_n(u)$ by:

$$P_{nm}(u) = \left(1 - u^2\right)^{m/2} \frac{d\,P_n(u)}{d\,u^m}.$$

The angles (φ, λ) are latitude and longitude with $\varphi \in (-90°, 90°)$, $\lambda \in (0, 360°)$, and the C_{nm}, S_{nm} are the Stokes coefficients, with $m \leq n$ and $n, m \in \mathbb{N}$. The standard convention

is to define $C_{00} = 1$ and $S_{n0} = 0$. The notation $J_n = -C_{n0}$ is also used for the remaining zonal terms, with $m = 0$. In addition, by the proper choice of the coordinate system through the center of mass of Mercury, the first order coefficients C_{10}, C_{11} and S_{11} vanish, the same is true for $C_{21} = S_{21} = 0$ if the axes of figure are aligned with the main axes of inertia. The effect of the perturbation on the rotation is therefore proportional to the size of the remaining zonal ($m = 0$), tesseral ($m < n$) and sectorial ($m = n$) terms. The remaining second order coefficients, $C_{20} = -J_2$ and C_{22}, can be related to the principal moments of inertia by:

$$J_2 m R^2 = C - \frac{(A+B)}{2}, C_{22} m R^2 = \frac{B-A}{4} \ .$$

It is a common practize to introduce the normalized polar moment of inertia c through the additional equation $C = cmR^2$.

The contributions H_K, H_R and V_G are given in different reference frames. To match them we aim to express both in an inertial frame, say e_0. For this reason we introduce the unit vector $(\hat{x}, \hat{y}, \hat{z})$, pointing from the center of mass of Mercury to the one of the Sun, which is defined in the body frame, say e_3, in terms of the angles (φ, λ) by the relations:

$$\hat{x} = \cos\varphi \cos\lambda, \quad \hat{y} = \cos\varphi \sin\lambda, \quad \hat{z} = \sin\varphi \ . \tag{6}$$

Together with the definition of P_n in terms of the sum

$$P_n(u) = \frac{1}{2^n} \sum_{k=0}^{[n/2]} \frac{(-1)^k (2n-2k)!}{k!(n-k)!(n-2k)!} u^{n-2k}$$

we find for $u = \sin\varphi$ the explicit form for P_{nm}, which are given by:

$$P_{nm}(\sin\varphi) = \frac{1}{2^n} \cos^m(\varphi) \sum_{k=0}^{[(n-m)/2]} \frac{(-1)^k (2n-2k)!}{k!(n-k)!(n-2k-m)!} \sin^{n-2k-m}(\varphi) \ . \tag{7}$$

Together with the formulae by Vieta (see e.g. Hazewinkel (2001))

$$\begin{matrix} \sin \\ \cos \end{matrix} (m\lambda) = \sum_{k=0}^{m} \left(\begin{matrix} m \\ k \end{matrix} \right) \cos^k \lambda \sin^{m-k} \lambda \begin{matrix} \sin \\ \cos \end{matrix} \left(\frac{1}{2}(m-k)\pi \right)$$

we find from Eq.(5), Eq.(6) and Eq.(7):

$$V = \frac{1}{r}\sum_{n=0}^{\infty}\sum_{m=0}^{n}\left(\frac{R}{r}\right)^{n}\left(C_{nm}\mathfrak{C}_{nm} + S_{nm}\mathfrak{S}_{nm}\right) \ . \tag{8}$$

For $n = 2$ the terms $\mathfrak{C}_{2m}$ turn out to be:

$$\mathfrak{C}_{20} = \frac{1}{2}\left(3\hat{z}^2 - 1\right) \ , \ \mathfrak{C}_{21} = 3\hat{x}\hat{z} \ , \ \mathfrak{C}_{22} = 3\left(\hat{x}^2 - \hat{y}^2\right) \ ,$$

and for $\mathfrak{S}_{2m}$ we find:

$$\mathfrak{S}_{20} = 0 \ , \ \mathfrak{S}_{21} = 3\hat{y}\hat{z} \ , \ \mathfrak{S}_{22} = 6\hat{x}\hat{y} \ .$$

The third order contributions, with $n = 3$ are

$$\mathfrak{C}_{30} = \frac{1}{2}\hat{z}\left(5\hat{z}^2 - 3\right) \ , \ \mathfrak{C}_{31} = \frac{3}{2}\hat{x}\left(5\hat{z}^2 - 1\right) \ , \ \mathfrak{C}_{32} = 15\hat{z}\left(\hat{x}^2 - \hat{y}^2\right) \ , \ \mathfrak{C}_{33} = 15\hat{x}\left(\hat{x}^2 - 3\hat{y}^2\right)$$

for $\mathfrak{C}_{3m}$, and

$$\mathfrak{S}_{30} = 0 \ , \ \mathfrak{S}_{31} = \frac{3}{2}\hat{y}\left(5\hat{z}^2 - 1\right) \ , \ \mathfrak{S}_{32} = 30\hat{x}\hat{y}\hat{z} \ , \ \mathfrak{S}_{33} = -15\left(\hat{y}^2 - 3\hat{x}^2\right) \ ,$$

for $\mathfrak{S}_{3m}$. In our study we are also interested in the fourth order contributions. For $n = 4$ we find for $\mathfrak{C}_{4m}$

$$\mathfrak{C}_{40} = \frac{1}{8}\left(3 - 30\hat{z}^2 + 35\hat{z}^4\right) \ , \ \mathfrak{C}_{41} = \frac{5}{2}\hat{x}\hat{z}\left(7\hat{z}^2 - 3\right) \ , \ \mathfrak{C}_{42} = -\frac{15}{2}\left(\hat{z}^2 + 2\hat{y}^2 - 1\right)\left(7\hat{z}^2 - 1\right) \ ,$$

$$\mathfrak{C}_{43} = 105\hat{x}\hat{z}\left(\hat{x}^2 - 3\hat{y}^2\right) \ , \ \mathfrak{C}_{44} = 105\left(\hat{x}^4 - 6\hat{x}^2\hat{y}^2 + \hat{y}^4\right) \ ,$$

and the terms $\mathfrak{S}_{4m}$ turn out to be of the form:

$$\mathfrak{S}_{40} = 0, \mathfrak{S}_{41} = \frac{5}{2}\hat{y}\hat{z}\left(7\hat{z}^2 - 1\right) \ , \mathfrak{S}_{42} = 15\hat{x}\hat{y}\left(7\hat{z}^2 - 1\right) \ ,$$

$$\mathfrak{S}_{43} = -105\hat{y}\left(\hat{y}^2 - 3\hat{x}^2\right) \ , \mathfrak{S}_{44} = 420\hat{x}\hat{y}\left(\hat{x}^2 - \hat{y}^2\right) \ .$$

Note, that in the above expressions, $\mathfrak{C}_{nm}$ and $\mathfrak{S}_{nm}$, it is possible to express one of the $(\hat{x}, \hat{y}, \hat{z})$ through the two others of them by making use of the relation Eq.(6), i.e. the fact that $\hat{x}^2 + \hat{y}^2 + \hat{z}^2 = 1$.

2.2. Matching the reference frames

To express the unit vector $(\hat{x}, \hat{y}, \hat{z})$ in e_0 we make use of the usual Andoyer angles (l, g, h) together with the angles (J, K); the angle J was already defined above, the angle K enters the projection of G on the inertial z-axis by $H = G\cos(K)$.

Let us denote by e_0 the inertial, by e_1 the orbital, by e_2 the spin and by e_3 the figure frame of references, respectively. The unit vector $(\hat{x}, \hat{y}, \hat{z})$, given in e_3, can be expressed in the spin frame e_2 by

$$(\hat{x}, \hat{y}, \hat{z})_{e_2} = M_1 \cdot (\hat{x}, \hat{y}, \hat{z})_{e_3}$$

with the matrix M_1 given by:

$$M_1 = \mathrm{diag}\left(\cos(g)\cos(l), \cos(g)\cos(J)\cos(l), \cos(J)\right) \ .$$

The transformed vector can be expressed in an inertial frame e_0 using the transformation

$$(\hat{x}, \hat{y}, \hat{z})_{e_0} = M_2 \cdot (\hat{x}, \hat{y}, \hat{z})_{e_2} \ ,$$

with

$$M_2 = \mathrm{diag}\left(\cos(h), \cos(h)\cos(K), \cos(K)\right) \ .$$

On the other hand, if the position of Mercury is given in the orbital frame e_1 it is also given in the inertial frame e_0 through:

$$(\hat{x}, \hat{y}, \hat{z})_{e_0} = M_3 \cdot (\cos(f), \sin(f), 0) \ ,$$

where f is the true anomaly of Mercury and the matrix M_3 is given by:

$$M_3 = \begin{pmatrix} \cos(\omega)\cos(\Omega) - \cos(i)\sin(\omega)\sin(\Omega) & -\cos(i)\cos(\omega)\sin(\Omega) - \cos(\Omega)\sin(\omega) & \sin(i)\sin(\Omega) \\ \cos(i)\cos(\Omega)\sin(\omega) + \cos(\omega)\sin(\Omega) & \cos(i)\cos(\omega)\cos(\Omega) - \sin(\omega)\sin(\Omega) & -\cos(\Omega)\sin(i) \\ \sin(i)\sin(\omega) & \cos(\omega)\sin(i) & \cos(i) \end{pmatrix} \ .$$

Here ω, Ω, i denote the argument of perihelion, longitude of ascending node, and inclination of Mercury, respectively. From the decompositions

$$M_1 = R_3(g)R_1(J)R_3(l),\ \ M_2 = R_3(h)R_1(K),\ \ M_3 = R_3(\Omega)R_1(i)R_3(\omega)$$

we are able to find

$$(\hat{x}, \hat{y}, \hat{z})_{e_3} = R_M \cdot (\cos(f), \sin(f), 0)\ ,$$

where we introduced the rotation matrix R_M being of the form:

$$R_M = R_3(-l)R_1(-J)R_3(-K)R_3(-h)R_3(\Omega)R_1(i)R_3(\omega)\ .$$

Together with the relations

$$\frac{a}{r} = 1 + 2\sum_{\nu=1}^{\infty} J_\nu(\nu e)\cos(\nu M)\ ,$$

$$\cos(f) = 2\frac{1-e^2}{e}\sum_{\nu=1}^{\infty} J_\nu(\nu e)\cos(\nu M) - e\ ,$$

$$\sin(f) = 2\sqrt{1-e^2}\sum_{\nu=1}^{\infty} \frac{dJ_\nu(\nu e)}{de}\frac{\sin(\nu M)}{\nu}\ ,$$

where J_ν are the Bessel functions of the first kind we are able to express the potential Eq.(8) in terms of the rotational and orbital elements only:

$$V = V(l, g, h, J, K, a, e, i, \omega, M). \tag{9}$$

It can also be expressed in terms of suitable action angle variables (l_i, L_i), with $i = 1, \ldots, 6$, using the set of modified Andoyer variables

$$\begin{aligned} (l_1,\ l_2,\ l_3) &= (l+g+h,\ -l,\ -h)\ , \\ (L_1,\ L_2,\ L_3) &= (G,\ G-L,\ G-H) = (G, G(1-\cos(J)),\ G(1-\cos(K))) \end{aligned} \tag{10}$$

for the rotational motion, and by making use of the classical Delaunay variables

$$
\begin{aligned}
(l_4,\ l_5,\ l_6) &= (M,\ \omega,\ \Omega)\ , \\
(L_4,\ L_5,\ L_6) &= \left(L_o,\ L_4\sqrt{1-e^2},\ L_5\cos(i)\right)
\end{aligned}
\qquad (11)
$$

for the orbital dynamics. In this setting the potential can be written in the form $V = V(l, L)$ with $l = (l_1, \ldots, l_6)$ and $L = (L_1, \ldots, L_6)$.

2.3. Simplifications and assumptions

The rotation period of Mercury, about $T_r = 58.6[d]$, and the orbital period around the sun, $T_o \simeq 87.9[d]$ lie close to the $3:2$ resonance ($2T_o \simeq 3T_r$). It is thus desirable to find a much simpler dynamical model, which reproduces the qualitative dynamics close to the resonance. We first introduce the change of coordinates

$$S_{3:2} : (l, L) \mapsto (\sigma, \Sigma)$$

with $\sigma = (\sigma_1, \ldots, \sigma_6)$, $\Sigma = (\Sigma_1, \ldots, \Sigma_6)$ defined by the generating function $S_{3:2}$ of the second kind

$$S_{3:2} = \Sigma_1 \left(l_1 - \frac{3}{2}l_4 - l_5 - l_6\right) + \Sigma_2 l_2 + \Sigma_3\,(l_3 + l_6) + \sum_{\kappa=4}^{6} \Sigma_\kappa l_\kappa\ .$$

In this setting the relevant resonant dynamics can be easily described in terms of the variables

$$
\begin{aligned}
&\sigma_1 = l_1 - \frac{3}{2}l_4 - l_5 - l_6\ ,\ \sigma_2 = l_2\ ,\ \sigma_3 = l_3 + l_6\ , \\
&\Sigma_1 = L_1\ ,\ \Sigma_2 = L_2\ ,\ \Sigma_3 = L_3\ ,
\end{aligned}
$$

while the remaining variables become:

$$2\Sigma_4 = 2L_4 + 3\Sigma_1\ ,\ \Sigma_5 = L_5 + \Sigma_1\ ,\ \Sigma_6 = L_6 + \Sigma_1 - \Sigma_3\ ,$$

and $\sigma_i = l_i$ with $i = 4, 5, 6$. In our first approach we aim to construct a simple resonant model, valid only close to exact resonance, by making use of the following assumptions:

i) we neglect the wobble motion of Mercury; we therefore set $J = 0$, which implies $L_2 = 0$ and reduces Eq.(3) to:

$$H_R = \frac{{\Sigma_1}^2}{2C} \tag{12}$$

ii) we neglect the effect of the rotation on the orbital dynamics, i.e. we investigate the dynamics on the reduced phase space

$$\frac{d\sigma_i}{dt} = \frac{\partial H}{\partial \Sigma_i} \ , \ \frac{d\Sigma_i}{dt} = -\frac{\partial H}{\partial \sigma_i} \ ,$$

with $i = 1, 3$, therefore assume that the orbital parameters $a, e, i, \omega, \Omega, M$ are known quantities, and $\Sigma_i = \Sigma_i(t), \sigma_i = \sigma_i(t)$ with $i = 4, 5, 6$ act as external time-dependent parameters on the dynamics of the reduced phase space.

iii) we neglect short periodic effects[1] and replace the potential V_G by its average over the mean anomaly of Mercury $M = l_4 = \sigma_4$:

$$\langle V \rangle \equiv \langle V_G \rangle_{\sigma_4} = \frac{1}{2\pi} \int_0^{2\pi} V_G(\sigma, \Sigma) d\sigma_4 \ .$$

As a result the averaged potential $\langle V \rangle$ becomes independent of σ_4, or the mean anomaly M, and thus the conjugated action Σ_4 becomes a constant of motion, and as a consequence the semi-major axis a is a constant too.

iv) we assume the presence of a perturbation leading to an additional precession of the nodes with constant precession rates, say $\dot{\omega}, \dot{\Omega} \neq 0$. In this setting we find for the remaining phase state variables, connected to the orbital motion, σ_5 and σ_6:

$$\frac{d\sigma_5}{dt} = \dot{\omega} \ , \ \frac{d\sigma_6}{dt} = \dot{\Omega} \ .$$

Note that since $\sigma_5 = \sigma_5(t) = \dot{\omega}t + \omega_0$ and $\sigma_6 = \sigma_6(t) = \dot{\Omega}t + \Omega_0$ the time dependent generating function $S_{3:2}$ leads to

$$\frac{\partial S_{3:2}}{\partial t} = -\Sigma_1 \dot{\omega} + (\Sigma_3 - \Sigma_1)\, \dot{\Omega}$$

[1] The effects within time scales, which are smaller than the revolution period of Mercury around the Sun.

which we have to add to our new Hamiltonian. The final resonant model takes the form

$$H_I = h_0 + \langle V \rangle \ , \tag{13}$$

with the new fundamental part:

$$h_0 = H_K + H_R - \Sigma_1 \dot{\omega} + (\Sigma_3 - \Sigma_1) \dot{\Omega} \tag{14}$$

and where H_K transforms into the new expression:

$$H_K = -\frac{m^3 \mu^2}{(2\Sigma_4 - 3\Sigma_1)^2} \ .$$

We derive from Eq.(14) the unperturbed angular frequencies:

$$\begin{aligned} \dot{\sigma}_1 &= \frac{\partial h_0}{\partial \Sigma_1} = \frac{\Sigma_1}{C} - \frac{3}{2} \frac{m^3 \mu^2}{\left(\Sigma_4 - \frac{3}{2}\Sigma_1\right)^3} - \dot{\omega} - \dot{\Omega} = \dot{l}_1 - \frac{3}{2} n - \dot{\omega} - \dot{\Omega} \ , \\ \dot{\sigma}_3 &= \frac{\partial h_0}{\partial \Sigma_3} = \dot{\Omega} \end{aligned}$$

since

$$\dot{\sigma}_4 = \frac{\partial h_0}{\partial \Sigma_4} = \frac{m^3 \mu^2}{\left(\Sigma_4 - \frac{3}{2}\Sigma_1\right)^3} \equiv n \ .$$

Here n is the mean motion of Mercury. For $\dot{\omega} = \dot{\Omega} = 0$ the spin-orbit resonance of Mercury translates into the commensurability:

$$2\dot{\sigma}_1 = 2\dot{l}_1 - 3\dot{\sigma}_4 \simeq 0 \ , \dot{\sigma}_3 - \dot{\sigma}_6 \simeq 0 \ ,$$

while for $\dot{\omega}, \dot{\Omega} \neq 0$ small frequency corrections due to the potential $\langle V \rangle$ have to be taken into account.

2.4. Workout of the time dependent resonant model

In the following discussion we limit our investigation to the contributions of the averaged potential, in which the Stokes coefficient in Table 1 are bigger than the threshold 10^{-7}, which

turn out to be $C_{20}, C_{22}, C_{30}, C_{40}$. According to this simplification the averaged potential $\langle V \rangle$ can be split into the form:

$$\langle V \rangle = C_{20} \langle V_{20} \rangle + C_{22} \langle V_{22} \rangle + C_{30} \langle V_{30} \rangle + C_{40} \langle V_{40} \rangle \ ,$$

where we used the notation $\langle V_{nm} \rangle$ to indicate the terms proportional to the coefficient C_{nm}. For the ongoing investigation we also need to separate the individual terms into purely resonant terms, just depending on σ_1, σ_3, and time dependent resonant terms through the presence of the additional angles $\sigma_5 = l_5 = \omega, \sigma_6 = l_6 = \Omega$, with $\omega = \omega(t), \Omega = \Omega(t)$. We use the short-hand notation:

$$\langle V_{nm} \rangle = \langle V_{nm} \rangle (\sigma_1, \sigma_3, l_5, l_6) = \langle v_{nm} \rangle (\sigma_1, \sigma_3) + \langle u_{nm} \rangle (\sigma_1, \sigma_3, l_5, l_6) \tag{15}$$

to indicate the dependency on the angles of the various terms.

The term $\langle V_{20} \rangle$:

The expression proportional to C_{20} in the unaveraged potential V_G takes the form:

$$\frac{R^2}{r^3} \mathfrak{C}_{20} = \frac{1}{2} \frac{R^2}{r^3} \left(3\hat{z}^2 - 1 \right) \ ,$$

which becomes after the average over the mean anomaly, and expanded up to 4th order in the orbital eccentricity e:

$$\langle V_{20} \rangle = -\frac{R^2 \left(8 + 12e^2 + 15e^4 \right)}{256a^3} \left([1]_{20} + [2]_{20} \cos{(\sigma_3)} + [3]_{20} \cos{(2\sigma_3)} \right) + O(e^5) \ .$$

The coefficients $[j]_{20}$, $j = 1, 2, 3$ are depending on Σ_1, Σ_3 through the inertial obliquity K, as well as on the orbital inclination i, and can be found in the Appendix. Note, that $\langle V_{20} \rangle = \langle v_{20} \rangle (\sigma_3)$ does not depend on σ_1 and is free of the angles l_5, l_6 up to $O(e)^5$ (i.e. $\langle u_{20} \rangle = 0$).

The term $\langle V_{22} \rangle$:

The expression proportional to C_{22} in V_G is of the form:

$$\frac{R^2}{r^3}\mathfrak{C}_{22} = 3\frac{R^2}{r^3}\left(\hat{x}^2 - \hat{y}^2\right) \ .$$

The averaged term up to $O(e^5)$ becomes:

$$\langle V_{22}\rangle = -\frac{R^2}{256a^3}\left(\langle v_{22}\rangle(\sigma_1,\sigma_3) + \langle u_{22}\rangle(\sigma_1,\sigma_3,l_5)\right) + O(e^5) \ ,$$

with

$$\langle v_{22}\rangle = E_1\left([1]_{22}\cos(2\sigma_1) + [2]_{22}\cos(2\sigma_1+\sigma_3) + \right.$$
$$\left.[3]_{22}\cos(2\sigma_1+2\sigma_3) + [4]_{22}\cos(2\sigma_1+3\sigma_3) + [5]_{22}\cos(2\sigma_1+4\sigma_3)\right) \ ,$$

where we collect the terms depending on the orbital eccentricity e by:

$$E_1 = e\left(-56 + 123e^2\right) \ .$$

The time dependent part of the expression is

$$\langle u_{22}\rangle = 318e^3\left([6]_{22}\cos(2\sigma_1+2l_5) + [7]_{22}\cos(2\sigma_1+\sigma_3+2l_5) + \right.$$
$$\left.[8]_{22}\cos(2\sigma_1+2\sigma_3+2l_5) + [9]_{22}\cos(2\sigma_1+3\sigma_3+2l_5) + [10]_{22}\cos(2\sigma_1+4\sigma_3+2l_5)\right) \ ,$$

where the coefficients $[1]_{22}\ldots[10]_{22}$, depending on the resonant actions, are given in the Appendix. Note, that $\langle v_{22}\rangle$ enters a term with the only resonant argument $2\sigma_1$, while the other Fourier modes are of the form

$$2\sigma_1 + k\sigma_3, k = 1,2,3,\ldots$$

up to order $O(e^4)$. The terms $\langle u_{22}\rangle = \langle u_{22}\rangle(\sigma_1,\sigma_3,l_5)$ do not depend on l_6 and contain terms of the form

$$2\sigma_1 + k\sigma_3 + 2l_5, k = 1,2,3,\ldots$$

with the additional argument $2l_5$.

The term $\langle V_{30} \rangle$:

The third order term proportional to C_{30} turns out to be:

$$\frac{R^3}{r^4}\mathfrak{C}_{30} = \frac{1}{2}\frac{R^3}{r^4}\hat{z}\left(5\hat{z}^2 - 3\right).$$

After the averaging no pure resonant terms survive ($\langle v_{30} \rangle = 0$) and $\langle V_{30} \rangle$ takes the form

$$\langle V_{30} \rangle = \frac{R^3}{128a^4}\left\langle u_{30} \right\rangle (\sigma_3, l_5)$$

with

$$\begin{aligned}
\langle u_{30} \rangle = E_2 \left([1]_{30} \sin\left(l_5 - 3\sigma_3\right) + [2]_{30} \sin\left(l_5 - 2\sigma_3\right) + \right.\\
[3]_{30} \sin\left(l_5 - \sigma_3\right) + [4]_{30} \sin\left(l_5\right) + [5]_{30} \sin\left(l_5 + \sigma_3\right) + \\
\left. [6]_{30} \sin\left(l_5 + 2\sigma_3\right) + [7]_{30} \sin\left(l_5 + 3\sigma_3\right)\right).
\end{aligned}$$

In the above expression the $[j]_{30}$, with $j = 1, \ldots 7$, label the third order coefficients, depending on the resonant actions, which are collected together in the Appendix. Moreover, we define

$$E_2 = e\left(2 + 5e^2\right)$$

to collect the contributions, which depend on the eccentricity. Note, that the time dependent terms $\langle u_{30} \rangle$ are again independent of l_6 (they only depend implicitly on it through the definition of σ_1, σ_3). We also conclude, that C_{30} does not contribute to the time independent resonant model, at the first order of masses approximation.

The term $\langle V_{40} \rangle$:

The expression proportonal to C_{40} of $\langle V_G \rangle_{\sigma_4}$ originates from the term

$$\frac{R^4}{r^5}\mathfrak{C}_{40} = \frac{1}{8}\frac{R^4}{r^5}\left(3 - 30\hat{z}^2 + 35\hat{z}^4\right) ,$$

and can again be split into

$$\langle V_{40}\rangle = \frac{R^4}{1024a^5}\left(\langle v_{40}\rangle(\sigma_3) + \langle u_{40}\rangle(\sigma_3, l_5)\right) \ .$$

Here the time-independent part is given by the expression:

$$\langle v_{40}\rangle = 4E_3\left([1]_{40} + [2]_{40}\cos(\sigma_3) + [3]_{40}\cos(2\sigma_3) + [4]_{40}\cos(3\sigma_3) + [5]_{40}\cos(4\sigma_3)\right) \ ,$$

where

$$E_3 = \left(1 + 5e^2\right) \ ,$$

and the time dependent contributions are:

$$\begin{aligned}\langle u_{40}\rangle = E_4\,([6]_{40}\cos(2l_5) + [7]_{40}\cos(2l_5 - 4\sigma_3) + [8]_{40}\cos(2l_5 - 3\sigma_3) +\\ [9]_{40}\cos(2l_5 - 2\sigma_3) + [10]_{40}\cos(2l_5 - \sigma_3) + [11]_{40}\cos(2l_5 + \sigma_3) +\\ [12]_{40}\cos(2l_5 + 2\sigma_3) + [13]_{40}\cos(2l_5 + 3\sigma_3) + [14]_{40}\cos(2l_5 + 4\sigma_3)) \ ,\end{aligned}$$

where

$$E_4 = e^2\left(2 + 7e^2\right)$$

(the coefficients $[\ldots]_{40}$ can be found again in the Appendix). Note, that $\langle v_{40}\rangle$ just depends on σ_3, while $\langle u_{40}\rangle$ depends on $\sigma_3, 2l_5$ but not on l_6.

To summarize, we find:

(i) The effect proportional to C_{20} (or J_2) is of order R^2/a^3, is time independent, and depending on the resonant angle σ_3 only.

(ii) The effect proportional to C_{22} can be split into time dependent as well as time independent terms: the time independent terms are proportional to eR^2/a^3, while the time dependent contributions are of order e^3R^2/a^3. The former contains a Fourier term depending just on the resonant argument $2\sigma_1$, while the later is depending on integer combinations of σ_1, σ_3 and l_5 only.

(iii) There is no time independent effect proportional to C_{30} (or J_3) on the averaged dynamics. Only time dependent terms, which are of order eR^3/a^4, and depending on integer combinations of σ_3 and l_5 contribute to it.

(iv) There is an important, time independent contribution, of order R^4/a^5, which is proportional to C_{40} and just depending on the resonant angle σ_3. The time dependent part of the potential is of order e^2R^4/a^5 only.

The preceeding list shows, that the time dependent effects are smaller than the time independent. For the numerical integration of the averaged system (see Sec.4) we are going to use the full potential of the form Eq.(15), while for the analytical study we are going to use the time independent part of the potential only.

3. Analytical treatment of the Cassini State 1

In this section, to obtain a simple analytical formula, we neglect the resonant terms in $\langle V\rangle$, which depend on time through $l_5 = \omega(t), l_6 = \Omega(t)$, and investigate the long-term dynamics close to $\sigma_1 = \sigma_3 = 0$. The potential $\langle V\rangle = \langle V\rangle(\sigma_1, \sigma_3)$ reduces to

$$\langle V\rangle(\sigma_1,\sigma_3) = C_{20}\langle v_{20}\rangle(\sigma_3) + C_{22}\langle v_{22}\rangle(\sigma_1,\sigma_3) + C_{40}\langle v_{40}\rangle(\sigma_3) \ ,$$

the integrable parts reduce to[2]

$$h_0 = H_K + H_R + (\Sigma_3 - \Sigma_1)\dot{\Omega} \ ,$$

and the new Hamiltonian model becomes:

$$H_{I0} = H_K + H_R + (\Sigma_3 - \Sigma_1)\dot{\Omega} + C_{20}\langle v_{20}\rangle + C_{22}\langle v_{22}\rangle + C_{40}\langle v_{40}\rangle \ . \tag{16}$$

The requirement to remain at the equilibrium is that $\dot{\Sigma}_1 = \dot{\Sigma}_3 = 0$ and translates into the set of equations:

$$\begin{aligned} f_1(\Sigma_1,\Sigma_3) &\equiv \left(\frac{\partial H_{I0}}{\partial \Sigma_1}\right)_{\sigma_1,\sigma_3=0} = 0 \ , \\ f_3(\Sigma_1,\Sigma_3) &= \left(\frac{\partial H_{I0}}{\partial \Sigma_3}\right)_{\sigma_1,\sigma_3=0} = 0 \ . \end{aligned} \tag{17}$$

[2]There is no need to keep $\dot{\omega}$ in the ongoing calculations.

The system can be solved for $\Sigma_1 = \Sigma_{1*}$, and $\Sigma_3 = \Sigma_{3*}$, which implies the 'equilibrium norm' of the angular momentum G_* and the 'equilibrium obliquity' K_*, which comes from the equations $\Sigma_{1*} = G_*$, $\Sigma_{3*} = \Sigma_{1*}\left(1 - \cos\left(K_*\right)\right)$. The physical interpretation of the equilibrium solution is the following: $\sigma_1 = 0$ means that the axis of smallest inertia points (on average) towards the Sun, $\sigma_3 = 0$ ensures that the node of the equator of Mercury is locked with the node of its orbit. While G_* defines a small correction of the unperturbed spin frequency, the angle K_* defines a specific value of the inertial obliquity. It translates to the usual called obliquity ϵ by the relation

$$\cos(\epsilon) = \cos(i)\cos(K) + \sin(i)\sin(K)\cos\left(\sigma_3 - \sigma_6\right) \ , \tag{18}$$

which reduces to

$$\epsilon_* = i - K_*$$

for $\sigma_3 = \sigma_6 = 0$.

The contributions $\langle v_{nm} \rangle$ depend on (Σ_1, Σ_3) through $s_K = s_K\left(\Sigma_1, \Sigma_3\right), c_K = c_K\left(\Sigma_1, \Sigma_3\right)$, since from $\Sigma_1 = L_1$, $\Sigma_3 = L_3$ we find $\Sigma_1 = G$, $\Sigma_3 = \Sigma_1(1 - \cos(K))$. We aim to express Eq.(17) in terms of (G, K) and thus have also to express the derivatives $\partial/\partial\Sigma_1$, $\partial/\partial\Sigma_3$ in terms of (G, K) too. A simple calculation shows for s_K and c_K and its derivatives:

$$\frac{\partial c_K}{\partial \Sigma_1} = \frac{1 - c_K}{G} \ , \ \frac{\partial c_K}{\partial \Sigma_3} = -\frac{1}{G} \ , \ \frac{\partial s_K}{\partial \Sigma_1} = \frac{c_K - 1}{G t_K} \ , \ \frac{\partial s_K}{\partial \Sigma_3} = \frac{1}{G t_K} \ ,$$

where we have introduced $t_K = \tan(K)$, and used the relation ${s_K}^2 + {c_K}^2 = 1$ and $0 \leq K \leq \pi/2$ to simplify the expressions. A long but straightforward calculation shows, that Eq.(17) can be written as:

$$\begin{aligned} f_1(G, K) &= -\frac{3n}{2} + \frac{G - C\dot{\Omega}}{C} + \frac{G_C M m}{G}\left(\frac{R^2}{a^3}\left([1]_{i_f} C_{20} + [2]_f C_{22}\right) + \frac{R^4}{a^5}[3]_f C_{40}\right) = 0 \ , \\ f_2(G, K) &= \dot{\Omega} + \frac{G_C M m}{G}\left(\frac{R^2}{a^3}\left([4]_f C_{20} + [5]_f C_{22}\right) + \frac{R^4}{a^5}[6]_f C_{40}\right) = 0 \ , \end{aligned} \tag{19}$$

with

$$\begin{aligned} [1]_f &= -\frac{3}{32}\left(8 + 12e^2 + 15e^4\right) s_{2(i-K)} t_{K/2} \ , \\ [2]_f &= -\frac{3}{8} e\left(-56 + 123e^2\right) c^3_{(i-K)/2} s_{(i-K)/2} t_{K/2} \ , \\ [3]_f &= \frac{15}{1024}\left(8 + 40e^2 + 105e^4\right)\left(2 s_{2(i-K)} + 7 s_{4(i-K)}\right) t_{K/2} \end{aligned}$$

and

$$
\begin{aligned}
[4]_f &= \frac{3}{32}\left(8+12e^2+15e^4\right) s_{2(i-K)}/s_K \ , \\
[5]_f &= \frac{3}{64} e\left(-56+123e^2\right)\left(2c_K s_i + s_{2(i-K)}\right)/s_K \ , \\
[6]_f &= -\frac{15}{1024}\left(8+40e^2+105e^4\right)\left(2s_{2(i-K)}+7s_{4(i-K)}\right)/s_K \ .
\end{aligned}
$$

Note, that we can use the second of Eq.(19) to eliminate G from the remaining equation to get:

$$
F(K) = -\left(\frac{3n}{2}+\dot{\Omega} c_K\right) + G_C M m \left(\frac{R^2}{a^3}\left([1]_F C_{20}+[2]_F C_{22}\right)+\frac{R^4}{a^5}[3]_F C_{40}\right) = 0 \ , \qquad (20)
$$

with

$$
\begin{aligned}
[1]_F &= -\frac{3}{32 s_K}\left(8+12e^2+15e^4\right) s_{2(i-K)} \ , \\
[2]_F &= -\frac{3}{64 C\dot{\Omega} s_K {s_{(i-K)/2}}^2} 3e\left(-56+123e^2\right) {s_{i-K}}^3 \ , \\
[3]_F &= \frac{15}{1024 C\dot{\Omega}}\left(8+40e^2+105e^4\right)\left(2s_{2(i-K)}+7s_{4(i-K)}\right) \ .
\end{aligned}
$$

Since the observed obliquities are usually rather small we substitute Eq.(18) for $\sigma_3 = \sigma_6 = 0$ in Eq.(20) and expand around $\epsilon = 0$ up to first order. Moreover we make use of the relations $C = cmR^2$ and $n^2 a^3 \simeq GM$ to get rid of some constants. Within these approximations we arrive at the simple formula:

$$
\begin{aligned}
\epsilon \ &= \left(1+\frac{2}{3}\frac{\dot{\Omega}}{n}\cos(i)\right) \times \qquad (21) \\
&\frac{c\dot{\Omega}\sin(i)}{n\left(2C_{22}\left(\frac{7}{2}e-\frac{123}{16}e^3\right)-C_{20}\left(1+\frac{3}{2}e^2+\frac{15}{8}e^4\right)+C_{40}\left(\frac{R}{a}\right)^2\left(\frac{5}{2}+\frac{25}{2}e^2+\frac{525}{16}e^4\right)-\frac{2}{3}\left(\frac{\dot{\Omega}}{n}\right)^2 c\sin(i)^2\right)} \ .
\end{aligned}
$$

Notice, that here the parameter $\dot{\Omega}$ is assumed to be negative, and that i is defined with respect to the plane, which minimizes the variations of the inclination. The formula coincides for $C_{40} = 0$ with Peale's formula up to $O(\dot{\Omega}/n)^2$ with the exception of the term $c\dot{\Omega}\cos(i)$ in

the denominator (Yseboodt & Margot 2006) [3]. However, a comparison of Eq.(21) with two different versions of Peale's formula clearly show the validity of the approach (see Fig.1): within the interval $c \in (0.3, 0.4)$ the predicted equilibrium obliquity at Cassini state 1 from Eq.(21) lies well within the value predicted with the formula in (Yseboodt & Margot 2006) and (Peale 1981) with a difference of about $10\epsilon^2 \simeq 600 mas$. Note that the parameter C_{30} is absent in this simple averaged model (there is however a time dependent effect as we will see below), the influence of C_{40} on the denominator is of the order of $O(R/a)^2 \simeq 4. \cdot 10^{-5}$, and $O(\dot{\Omega}/n)^2 \simeq 8. \cdot 10^{-7}$ does not modify the results. For the parameters given in Table 1 the equilibrium obliquity for Mercury turns out to be $\epsilon = 2.02'$.

We conclude the section with a short summary of the assumptions, which were made to obtain Eq.(21): i) zero wobble, ii) only the coupling of the spin on the orbit was taken into account, iii) short periodic effects are neglected (average over mean orbital motion and time), iv) the orbital parameters are kept constant but then we assume a constant rate of regression of the ascending node. The resulting accuracy of the formula can be quantified as follows: 1) for the average a 4th order expansion in eccentricty e was taken into account (error $O(e^5) \simeq 3. \cdot 10^{-4}$), 2) time dependent resonant terms are neglected (with this we set $d\epsilon/dt = 0$), 3) a first order expansion in obliquity ϵ allowed to make the formula explicit and induced an aditional error of $O(\epsilon^2) \simeq 1. \cdot 10^{-3}$.

This formula and Peale's formula as well are lacking of the fact, that the obliquity changes with time not only because $\dot{\Omega}$ is not a constant but because the 'equilibrium' conditions $\sigma_1 = \sigma_3 = 0$ cannot be fulfilled for all times. As we have seen, even for constant precession rates, the Hamiltonian is not a conserved quantity, i.e. for a Hamiltonian of the form $H = H(\Sigma_1, \Sigma_3, \sigma_1, \sigma_3, t)$ we cannot deduce that $\sigma_1 = \sigma_2 = 0$ for all times, since

$$\dot{\sigma}_{1,2} = \frac{\partial H(\Sigma_1, \Sigma_3, \sigma_1, \sigma_3, t)}{\partial \Sigma_{1,2}} \rightarrow \dot{\sigma}_{1,2} \neq 0 \ ,$$

and therefore $\sigma_{1,2}$ are subject to change too. A second (and probably more visible) concern of formulas of the type Eq.(21) is the fact, that the resulting ϵ strongly depends on the choice of the reference plane to which the orbital inclination i and in which the average precession rate $\dot{\Omega}$ are defined. To optimize the result, the reference plane should be the plane to which

[3]For small $(\dot{\Omega}/n)$ it is possible to simplify the calculations by setting $G = n_s C \simeq \frac{3}{2} nC$ in the second of Eq.(19), expanding up to 1st order in ϵ close to $\epsilon = 0$. The resulting formula for ϵ coincides with Eq.(21) up to $O(\dot{\Omega}/n)^2$. The additional terms are therefore stemming from the small spin frequency correction, not taken into account in (Peale 1981).

the variations in i become minimal, which can be seen as a generalization to the so-called Laplace plane (not to be confused with the invariant Laplace plane, the plane normal to the angular momentum of the complete system). In the next Section we present a possible solution to these kind of problems.

4. The secular variations of the orbital elements

We use a similar approach as in (Noyelles & D'Hoedt 2012). In a reference frame based on the ecliptic at J2000, we define averaged eccentricities and inclinations (Noyelles & D'Hoedt 2012) as:

$$\begin{aligned}
h(t) &= -7.76651 \times 10^{-11} t^2 + 1.43999 \times 10^{-6} t + 0.200722, && (22)\\
k(t) &= -2.31417 \times 10^{-11} t^2 - 5.52628 \times 10^{-6} t + 0.0446629, && (23)\\
p(t) &= 2.38036 \times 10^{-16} t^3 - 9.03918 \times 10^{-12} t^2 - 1.27635 \times 10^{-6} t + 0.0456355, && (24)\\
p(t) &= -1.04673 \times 10^{-11} t^2 - 1.27792 \times 10^{-6} t + 0.0456362, && (25)\\
q(t) &= 2.52407 \times 10^{-16} t^3 - 1.06586 \times 10^{-11} t^2 + 6.54322 \times 10^{-7} t + 0.0406156, && (26)\\
q(t) &= -1.21729 \times 10^{-11} t^2 + 6.52656 \times 10^{-7} t + 0.0406163, && (27)
\end{aligned}$$

with $h(t) = e(t)\sin\varpi(t)$, $k(t) = e(t)\cos\varpi(t)$, $p(t) = \sin\left(\frac{I(t)}{2}\right)\sin\Omega(t)$ and $q(t) = \sin\left(\frac{I(t)}{2}\right)\cos\Omega(t)$, the time origin begin J2000 and the time unit being the year. I is the orbital inclination of Mercury defined with respect to the ecliptic at J2000. These are fits over the duration of the JPL DE406 ephemerides, i.e. 6,000 years. For the inclination variables, 2 fits are given: the third-order fit (Eq.24 and Eq.26) is more accurate, but the second-order one is easier to extrapolate into a trigonometric decomposition.

From these formulae we extract trigonometric expressions:

$$\begin{aligned}
h(t) &= 0.1990903983\sin\varpi_1(t) + 0.01094807206\sin\varpi_2(t), && (28)\\
k(t) &= 0.1990903983\cos\varpi_1(t) + 0.01094807206\cos\varpi_2(t), && (29)\\
p(t) &= 0.06094690052\sin\Omega_1(t) + 0.01442538649\sin\Omega_2(t), && (30)\\
q(t) &= 0.06094690052\cos\Omega_1(t) + 0.01442538649\cos\Omega_2(t), && (31)
\end{aligned}$$

with

$$\varpi_1(t) = 2.852011398 \times 10^{-5} t + 1.30845314198, \qquad (32)$$

$$\begin{aligned}
\varpi_2(t) &= 4.767836272 \times 10^{-6} t + 2.26085090227, & (33)\\
\Omega_1(t) &= -2.298222197 \times 10^{-5} t + 0.60658814513, & (34)\\
\Omega_2(t) &= 1.340719884 \times 10^{-5} t + 2.28580288184. & (35)
\end{aligned}$$

Using trigonometric series make the orbital solutions easy to extrapolate without divergence. We extrapolate them over several millions of years to optimize their numerical identification, and we assume that the solution is close to the real one over the validity of the DE406 ephemerides. This assumption will be checked a posteriori (Sect.5.1).

We can now plug these new orbital elements in the equations of the averaged rotational dynamics of Mercury. Using Laskar's frequency analysis (Laskar 1999, 2005), we express the ecliptic obliquity K and the resonant argument σ_3 with a quasiperiodic decomposition such as

$$\begin{aligned}
K(t) &= I(t) + \sum a_i \cos \omega_i t + \phi_i, & (36)\\
\sigma_3(t) &= \sum b_j \cos \omega_j t + \phi_j, & (37)
\end{aligned}$$

a_i and b_j being real amplitudes, $\omega_{i,j}$ frequencies, and $\phi_{i,j}$ phases at $t = 0$. The frequencies can either come from the forced motion, and so are combinations of the ones present in the orbital motion (Eq.32 to Eq.35), or are due to free librations, that are expected to be damped. Their presence in the numerical outputs comes from a non optimal choice of the initial conditions. Our first run with $C_{20} = -5.031 \times 10^{-5}$, $C_{22} = 8 \times 10^{-6}$, $C_{30} = -1.188 \times 10^{-5}$, $C_{40} = -1.95 \times 10^{-5}$ and $C = 0.35mR^2$ yields the Tab.2.

The frequency analysis giving this table has been performed over 7.95 Myr with 4,096 points equally spaced by 1,942.5 years. The free librations should have periods of ≈ 15 years in longitude and $\approx 1,000$ years in obliquity (D'Hoedt & Lemaitre 2004; Rambaux & Bois 2004), these periods should appear aliased, while the forced perturbations should not since their periods should be bigger than 10,000 years. We then optimize the initial conditions iteratively in removing the free librations, as described in (Noyelles et al. 2013). These free oscillations act as a noise in the determination of the forced ones, that explains for instance small discrepancies in the periods. Refining these initial conditions improves the accuracy of the determination of the forced oscillations.

Table 2: An example of frequency analysis of the numerical outputs of our system.

N	Amplitude (arcmin)	Period (y)	Identification
$K-I$			
1	1.9755	∞	$< K-I >$
2	0.2682	172,665.2	$\Omega_2-\Omega_1$
3	0.0592	86,332.6	$2\Omega_2-2\Omega_1$
4	0.0254	264,530.5	$\omega_1-\omega_2$
5	0.0132	60,999.1	$2\omega_1-2\Omega_1$
6	0.0121	57,555.3	$3\Omega_2-3\Omega_1$
7	0.0026	4,167.1	free
8	0.0025	43,166.2	$4\Omega_2-4\Omega_1$
9	0.0025	4,302.6	free
σ_3			
1	6.2509	172,665.2	$\Omega_2-\Omega_1$
2	1.4683	86,332.6	$2\Omega_2-2\Omega_1$
3	0.3462	57,555.1	$3\Omega_2-3\Omega_1$
4	0.1112	60,999.0	$2\omega_1-2\Omega_1$
5	0.0816	43,166.3	$4\Omega_2-4\Omega_1$
6	0.0400	497,291.8	$\varpi_2-\varpi_1+\Omega_2-\Omega_1$
7	0.0396	104,473.0	$\varpi_1-\varpi_2+\Omega_2-\Omega_1$
8	0.0261	45,075.0	$2\varpi_1-3\Omega_1+\Omega_2$
9	0.0214	4,167.1	free
10	0.0209	4,302.6	free

4.1. Fitting the initial conditions

The goal is to find relevant initial conditions for any set of interior parameters $(C_{20}, C_{22}, C_{30}, C_{40}, C)$ consistent with the observations and the theory. For that, we consider 56 different cases (Tab.3).

Table 3. Our 56 sets of possible interior parameters.

N	C_{20} ($\times 10^{-5}$)	C_{22} ($\times 10^{-6}$)	C_{30} ($\times 10^{-5}$)	C_{40} ($\times 10^{-5}$)	$C/(mR^2)$
0	−5.031	8.088	−1.188	−1.95	0.35
1	−5.031	8.	−1.188	−1.95	0.35
2	−5.031	8.02	−1.188	−1.95	0.35
3	−5.031	8.04	−1.188	−1.95	0.35
4	−5.031	8.06	−1.188	−1.95	0.35
5	−5.031	8.08	−1.188	−1.95	0.35
6	−5.031	8.1	−1.188	−1.95	0.35
7	−5.031	8.12	−1.188	−1.95	0.35
8	−5.031	8.14	−1.188	−1.95	0.35
9	−5.031	8.16	−1.188	−1.95	0.35
10	−5.031	8.18	−1.188	−1.95	0.35
11	−5.031	8.2	−1.188	−1.95	0.35
12	−5.1	8.088	−1.188	−1.95	0.35
13	−5.08	8.088	−1.188	−1.95	0.35
14	−5.06	8.088	−1.188	−1.95	0.35
15	−5.04	8.088	−1.188	−1.95	0.35
16	−5.02	8.088	−1.188	−1.95	0.35
17	−5.	8.088	−1.188	−1.95	0.35
18	−4.98	8.088	−1.188	−1.95	0.35
19	−4.96	8.088	−1.188	−1.95	0.35
20	−4.94	8.088	−1.188	−1.95	0.35
21	−4.92	8.088	−1.188	−1.95	0.35
22	−4.9	8.088	−1.188	−1.95	0.35
23	−5.031	8.088	−1.188	−1.71	0.35
24	−5.031	8.088	−1.188	−1.76	0.35
25	−5.031	8.088	−1.188	−1.81	0.35
26	−5.031	8.088	−1.188	−1.86	0.35
27	−5.031	8.088	−1.188	−1.91	0.35
28	−5.031	8.088	−1.188	−1.96	0.35
29	−5.031	8.088	−1.188	−2.	0.35
30	−5.031	8.088	−1.188	−2.05	0.35

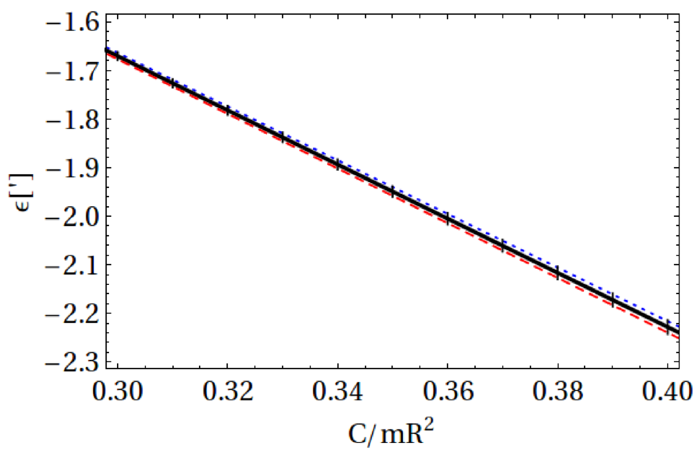

Fig. 1.— Relation between normalised polar moment of inertia $c = C/mR^2$ versus observed obliquity ϵ in arcminutes. We compare the new formula Eq.(21) - black (thick) - with the usual one Eq.(1) - red (dashed) - and with Eq.(4) of Peale (1981) - blue (dotted) - within in the interval $0.3 \leq c \leq 0.4$ for the actual parameters of Mercury.

For each of them, a numerical study has been performed as explained above. After refinement of the initial conditions that gave us an accurate frequency decomposition of the signals, we identified 34 amplitudes, i.e. we can now write:

$$
\begin{aligned}
K &= I + a_1 - 2a_2\cos(\Omega_2-\Omega_1) + 2a_3\cos(2\Omega_2-2\Omega_1) - 2a_4\cos(\varpi_1-\varpi_2) \\
&+ 2a_5\cos(2\varpi_1-2\Omega_1) - 2a_6\cos(3\Omega_2-3\Omega_1) + 2a_7\cos(4\Omega_2-4\Omega_1) \\
&+ 2a_8\cos(\varpi_2-\varpi_1+\Omega_2-\Omega_1) + 2a_9\cos(\varpi_1-\varpi_2+\Omega_2-\Omega_1) + 2a_{10}\cos(\varpi_1+\varpi_2-2\Omega_1) \\
&- 2a_{11}\cos(2\varpi_1-3\Omega_1+\Omega_2) - 2a_{12}\cos(5\Omega_2-5\Omega_1) + 2a_{13}\cos(2\varpi_1-2\varpi_2) \\
&- 2a_{14}\cos(\varpi_1-\varpi_2-2\Omega_1+2\Omega_2) - 2a_{15}\cos(\varpi_2-\varpi_1-2\Omega_1+2\Omega_2) \\
&- 2a_{16}\cos(2\varpi_1-2\Omega_2), \qquad (38) \\
\sigma_3 &= 2a_{17}\sin(\Omega_2-\Omega_1) - 2a_{18}\sin(2\Omega_2-2\Omega_1) + 2a_{19}\sin(3\Omega_2-3\Omega_1) \\
&- 2a_{20}\sin(2\varpi_1-2\Omega_1) - 2a_{21}\sin(4\Omega_2-4\Omega_1) - 2a_{22}\sin(\varpi_2-\varpi_1+\Omega_2-\Omega_1) \\
&- 2a_{23}\sin(\varpi_1-\varpi_2+\Omega_2-\Omega_1) + 2a_{24}\sin(2\varpi_1-3\Omega_1+\Omega_2) + 2a_{25}\sin(5\Omega_2-5\Omega_1) \\
&+ 2a_{26}\sin(2\varpi_1-\Omega_1-\Omega_2) - 2a_{27}\sin(\varpi_1+\varpi_2-2\Omega_1) + 2a_{28}\sin(-\varpi_1+\varpi_2-2\Omega_1+2\Omega_2) \\
&+ 2a_{29}\sin(\varpi_1-\varpi_2-2\Omega_1+2\Omega_2) - 2a_{30}\sin(2\varpi_1-4\Omega_1+2\Omega_2) - 2a_{31}\sin(6\Omega_2-6\Omega_1) \\
&+ 2a_{32}\sin(\varpi_1+\varpi_2-3\Omega_1+\Omega_2) - 2a_{33}\sin(\varpi_1-\varpi_2-3\Omega_1+3\Omega_2) \\
&- 2a_{34}\sin(\varpi_2-\varpi_1-3\Omega_1+3\Omega_2), \qquad (39)
\end{aligned}
$$

with

$$a_i = \frac{C/(mR^2)}{\alpha C/(mR^2)+\beta C_{20}+\gamma C_{22}+\delta} \qquad (40)$$

for $i = 1, 2, 5, 6, 17, 18, 19, 20, 21, 22, 23, 24, 26, 27$,

$$a_i = \frac{C/(mR^2)}{\alpha+\beta C_{20}+\gamma C_{22}} \qquad (41)$$

for $i = 3, 4$

$$a_i = \frac{C/(mR^2)}{\alpha+\beta C_{20}} \qquad (42)$$

for $i = 7, 8, 9, 10, 11, 12, 13, 14, 15, 16, 34$, and

$$a_i = \frac{C/(mR^2)}{\alpha C/(mR^2)+\beta C_{20}+\gamma} \qquad (43)$$

Table 3—Continued

N	C_{20} ($\times 10^{-5}$)	C_{22} ($\times 10^{-6}$)	C_{30} ($\times 10^{-5}$)	C_{40} ($\times 10^{-5}$)	$C/(mR^2)$
31	-5.031	8.088	-1.188	-2.1	0.35
32	-5.031	8.088	-1.188	-2.15	0.35
33	-5.031	8.088	-1.188	-2.19	0.35
34	-5.031	8.088	-1.188	-1.95	0.32
35	-5.031	8.088	-1.188	-1.95	0.326
36	-5.031	8.088	-1.188	-1.95	0.332
37	-5.031	8.088	-1.188	-1.95	0.338
38	-5.031	8.088	-1.188	-1.95	0.344
39	-5.031	8.088	-1.188	-1.95	0.349
40	-5.031	8.088	-1.188	-1.95	0.356
41	-5.031	8.088	-1.188	-1.95	0.362
42	-5.031	8.088	-1.188	-1.95	0.368
43	-5.031	8.088	-1.188	-1.95	0.374
44	-5.031	8.088	-1.188	-1.95	0.38
45	-5.031	8.088	-1.3	-1.95	0.35
46	-5.031	8.088	-1.28	-1.95	0.35
47	-5.031	8.088	-1.26	-1.95	0.35
48	-5.031	8.088	-1.24	-1.95	0.35
49	-5.031	8.088	-1.22	-1.95	0.35
50	-5.031	8.088	-1.2	-1.95	0.35
51	-5.031	8.088	-1.18	-1.95	0.35
52	-5.031	8.088	-1.16	-1.95	0.35
53	-5.031	8.088	-1.14	-1.95	0.35
54	-5.031	8.088	-1.12	-1.95	0.35
55	-5.031	8.088	-1.1	-1.95	0.35

for $i = 25, 28, 29, 30, 31, 32, 33$.

The idea of these formulae come from Peale's formula (Eq.1 & Eq.21). We hoped to get amplitudes alike

$$a_i = \frac{C/(mR^2)}{\alpha C/(mR^2) + \beta C_{20} + \gamma C_{22} + \zeta C_{30} + \phi C_{40} + \eta}. \tag{44}$$

For that, we tried to fit amplitudes with respect to one parameter, i.e.

$$f\left(\frac{C}{mR^2}\right) = \frac{aC/\left(mR^2\right)}{1 + bC/\left(mR^2\right)} \tag{45}$$

when possible and

$$f\left(\frac{C}{mR^2}\right) = aC/\left(mR^2\right) \tag{46}$$

when not, and also

$$f\left(C_{20}\right) = \frac{1}{a + bC_{20}}, \tag{47}$$

$$f\left(C_{22}\right) = \frac{1}{a + bC_{22}}, \tag{48}$$

$$f\left(C_{30}\right) = \frac{1}{a + bC_{30}}, \tag{49}$$

$$f\left(C_{40}\right) = \frac{1}{a + bC_{40}}. \tag{50}$$

It turned out that it was impossible to estimate the influence of C_{30} and C_{40} with enough reliability, that is the reason why they do not appear in the final formulae (Eq.40 to 43). The coefficients used are gathered in Tab.4.

5. The influence of the different effects

The derivation of these new formulae for the obliquity of Mercury allows us to estimate the influence of usually neglected effects, like the secular variations of the orbital elements,

the tides and the higher order harmonics. For that we first need to test the reliability of our initial conditions on a real, non-averaged simulation of the rotation of Mercury.

5.1. Differences between the averaged and the unaveraged system

We proceed as in (Noyelles & D'Hoedt 2012), Sect.4. To simulate the non-averaged rotation of Mercury, we integrate numerically the equations related to the following Hamiltonian:

$$\begin{aligned}\mathcal{H} &= \frac{n}{2(1-\delta)}(P^2-3\delta P) \\ &- \frac{3}{2}\frac{GM}{nd^3}\left(\epsilon_1\left(x^2+y^2\right)+\epsilon_2\left(x^2-y^2\right)+\epsilon_3\left(\frac{R}{d}\right)z(5z^2-3)+\epsilon_4\left(\frac{R}{d}\right)^2(3-30z^2+35z^4)\right),\end{aligned} \tag{51}$$

with $\epsilon_1 = -C_{20}mR^2/C$, $\epsilon_2 = 2C_{22}mR^2/C$, $\epsilon_3 = C_{30}mR^2/(2C)$, $\epsilon_4 = C_{40}mR^2/(8C)$, $\delta = 1-C_m/C$, C_m being the polar inertial momentum of the mantle of Mercury, P is the norm of the angular momentum normalized by nC, d is the Sun-Mercury distance, and x and y are the first two coordinates of the unit vector pointing to the Sun in a reference frame defined by the principal axes of inertia of Mercury. The canonical variables associated with this Hamilltonian are

$$\begin{array}{ll} l_1, & P = \frac{L_1}{nC}, \\ l_3, & R = \frac{L_3}{nC}, \end{array}$$

the Hamilton equations associated being

$$\begin{array}{ll} \frac{dl_1}{dt} = \frac{\partial\mathcal{H}}{\partial P}, & \frac{dP}{dt} = -\frac{\partial\mathcal{H}}{\partial l_1}, \\ \frac{dl_3}{dt} = \frac{\partial\mathcal{H}}{\partial R}, & \frac{dR}{dt} = -\frac{\partial\mathcal{H}}{\partial l_3}. \end{array}$$

The position of the Sun with respect to Mercury is computed using JPL DE406 ephemerides, so it contains every perturbation, i.e. not only the secular, but also the planetary ones. Inappropriate initial conditions in the numerical integration of the equations would yield unexpected free oscillations. The free longitudinal oscillations, their period being ≈ 12 years, can be easily damped adiabatically over 5,000 years, the DE406 ephemerides starting at -3,000. However, the free oscillations in obliquity, whose period is about 1,000 years, cannot

be damped over such a timescale without a significant and artificial impact on the equilibrium. So, we add a damping only on the longitudinal motion, and we get free oscillations in obliquity as in Fig.2. This obliquity is the actual obliquity ϵ, it is equal to $K - I$ only if $\sigma_3 = 0$. We obtain it with

$$\cos\epsilon = \frac{\vec{G}\cdot\vec{n}}{||\vec{G}||}. \tag{52}$$

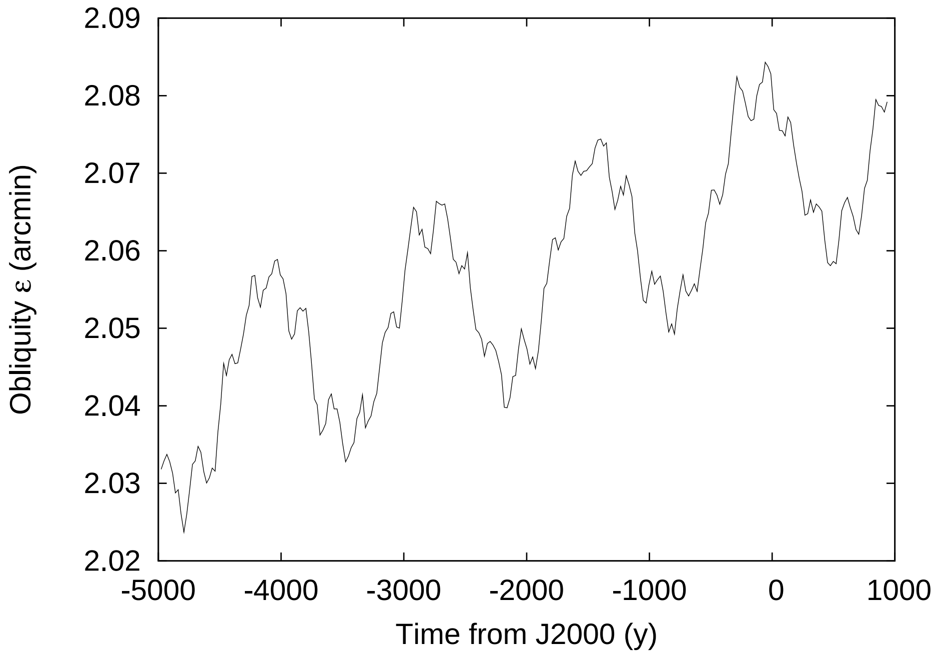

Fig. 2.— Obliquity ϵ of Mercury given by the unaveraged system, with $C_{20} = -5.031 \times 10^{-5}$, $C_{22} = 8.088 \times 10^{-6}$, $C_{30} = C_{40} = 0$ and $C = 0.35mR^2$. The $\approx$ 1,000 years oscillations are free librations that would not be present if the initial conditions were ideal.

The amplitude of the free oscillations can be seen as an estimation of the error due to the initial conditions. This error can come from all the approximations made in the averaging process, in particular the limitation to a first order averaging, the expansions in eccentricity, or the exclusion of the planetary perturbations. The Fig.3 shows the amplitude of these oscillations for different values of the interior parameters C_{20}, C_{22} and C, the other ones not affecting our initial conditions. These amplitudes have been obtained thanks to a frequency analysis. We can see that the amplitude of the free oscillations are always smaller than 750 milli-arcsec. Margot et al. (2012) derived from observations a moment of inertia $C = 0.346mR^2$, so the amplitude of the free oscillations should be $\approx$ 650 milli-arcsec. This

is the theoretical error induced by the Eq.38 and Eq.39.

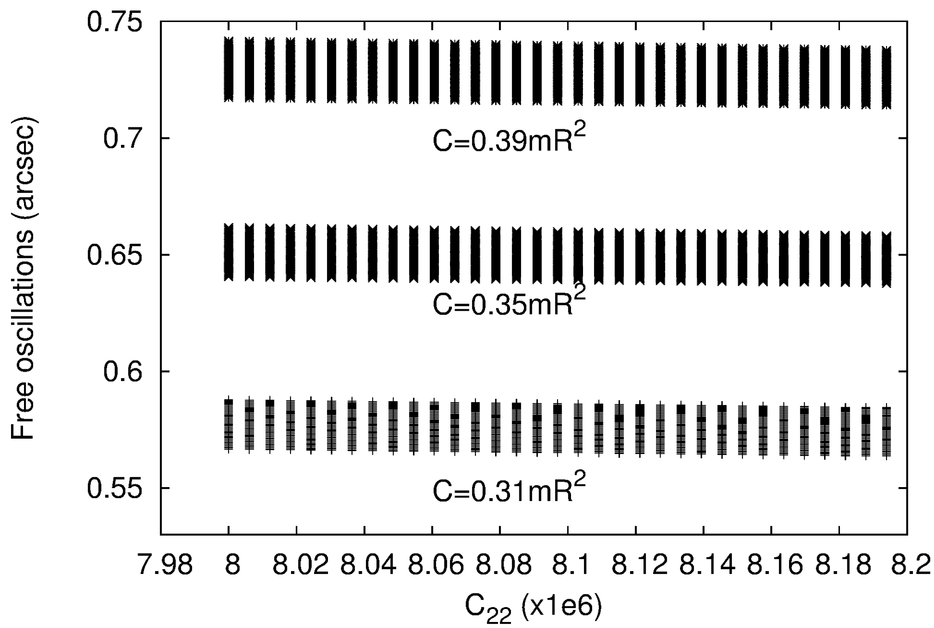

Fig. 3.— Amplitude of the free oscillations, induced by our initial conditions.

5.2. Influence of J_3

We failed to find an influence of $C_{30} = -J_3$ in our numerical and analytical formulae of the equilibrium obliquity. Anyway, this parameter is present in the full equations of the rotational dynamics of the system, and we checked its influence in plotting the average value of the obliquity ϵ with respect to J_3 (Fig.4).

In Fig.4 we clearly see the influence of C_{30} on the obliquity ϵ, which we did not see in the simple analytical nor the single averaged but still time dependent model. As we learned from (iii) of Sect.2.4, there is a time-dependent contribution proportional to C_{30} of the order of eR^3/a^4, which is affecting the action Σ_3 - thus the inertial obliquity K as well as ϵ through the presence of the resonant argument σ_3 and the argument of the perihelion ω. However, the effect is very small due to the presence of the a^4 in the denominator and can safely be neglected for the same reasoning we did to explain why J_4 does not influence the results.

A linear fit gives

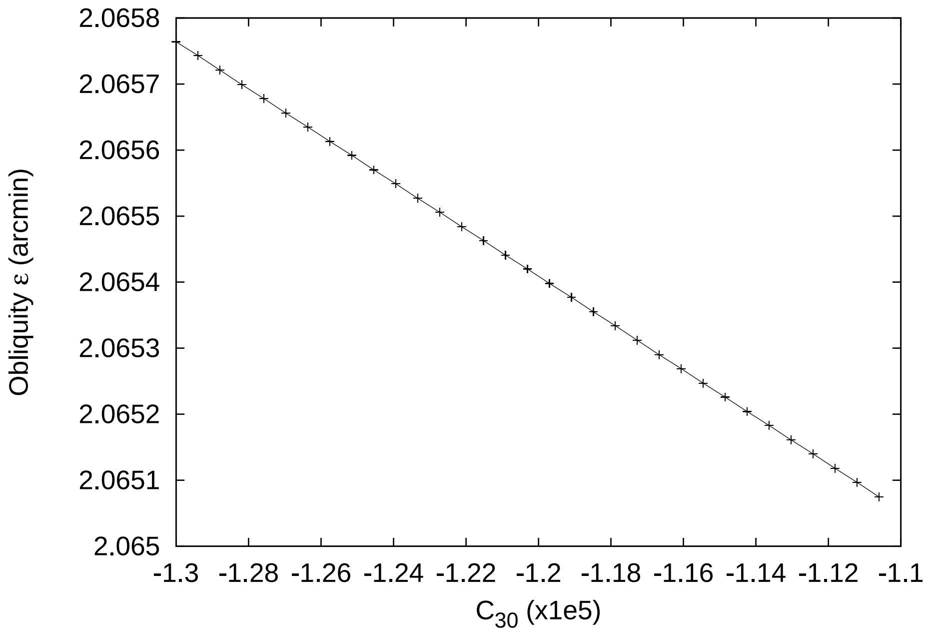

Fig. 4.— Influence of C_{30} on the mean obliquity, obtained after numerical integration of the non-averaged equations. This has been computed from the cases 45 to 55 (Tab.3).

$$\epsilon = (-355.197 C_{30} + 2.06115) \quad \text{arcmin}, \tag{53}$$

so neglecting J_3 should induce an error of ≈ 253 mas for $J_3 = 1.188 \times 10^{-5}$. We did the same job for J_4 without finding any reliable influence.

From a theoretical point of view the difference between the averaged (but still time dependent) and original system of equations of motion can be seen in the following way: with the average over the mean orbital longitude we neglect not only the fast periodic effects (the relevant timescale being the orbital period of Mercury), but we also set the orbital distance of Mercury from the Sun to a constant value. Thus, in the averaged system, we are unable to include all the perturbations, which affect the time evolution of the semimajor axis of the planet. In addition we needed to expand the potential into a truncated powerseries to be able to introduce the resonant argument and perform the averaging over the fast angle. Since we have limited all our expansions to the 4th order in eccentricity, an additional difference of the order $\mathcal{O}(e^5)$ is expected. Last but not least, we use the simple average rule, which is equivalent to a first order averaging in the ratio of the masses m/M (the mass of Mercury over the mass of the Sun).

5.3. The tides

The shape of Mercury, if hydrostatic, is due to the influence of a centrifugal potential, due to Mercury's spin, and a tidal potential. This tidal potential can be split into a static and an oscillating potential, as a consequence the gravity field parameters C_{20} and C_{22} and the polar momentum of inertia C should experience periodic variations alike (Rappaport et al. 2008; Van Hoolst et al. 2008):

$$
\begin{aligned}
C_{20}(t) &= C_{20}^{static} + \frac{k_2}{2} q_t e \cos(l_4 - l_5 - l_6), &(54)\\
C_{22}(t) &= C_{22}^{static} - \frac{k_2}{4} q_t e \cos(l_4 - l_5 - l_6), &(55)\\
C(t) &= C^{static} - \frac{k_2}{3} q_t e M R^2 \cos(l_4 - l_5 - l_6), &(56)
\end{aligned}
$$

where k_2 is the classical Love number, e the eccentricity of Mercury, and $l_4 - l_5 - l_6$ represents the mean anomaly of Mercury. We also have

$$q_t = -3\frac{M}{m}\left(\frac{R}{a}\right)^3, \tag{57}$$

where M is the mass of the Sun, m the mass of Mercury, R its mean radius and a its semi-major axis. With $e = 0.2056$, $a = 57,909,226.5415$ m (JPL HORIZONS), $M/m = 6.0239249 \times 10^6$ and $R = 2439.7$ km (Archinal et al. 2011), we have $q_t e = -2.778369 \times 10^{-7}$. The Love number k_2 should be between 0 (fully inelastic rigid Mercury) and 1.5 (fully fluid Mercury). We think, from the detection of the longitudinal librations of Mercury, that it should be closer to a rigid body than to a fluid one, so we consider $k_2 = 0.5$. The results are given in Fig.5. We can see a peak-to-peak variation of $\approx$ 100 mas. We can also see the secular drift due to the variations of the orbital elements related to eccentricity and inclination, $\approx$ 10 mas over 20 years.

5.4. Summary

The influence of the different effects is gathered in the Tab.5. The free librations that are mentioned are generated by the lack of accuracy of our initial conditions (Eq.38 & 39), they do not have any physical relevance. We have made the assumptions that they have been damped to a negligible amplitude, as suggested by Peale (2005). The other effects are smaller than that, they all have been estimated in this study except the polar motion, coming from

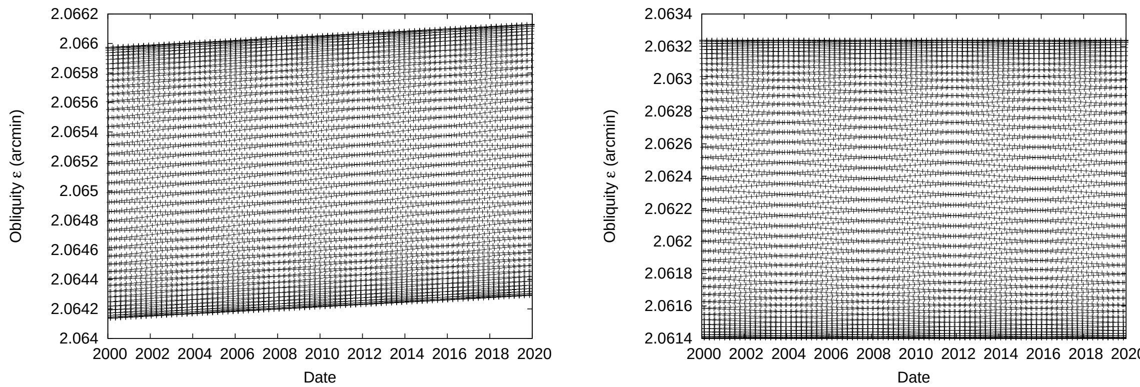

Fig. 5.— Variations of the obliquity of Mercury due to tides, with the numerical formula (left), and the analytical one (right). The period of variation is the orbital period, i.e. 88 days.

(Noyelles et al. 2010), and the amplitude of the short-period librations, from (Dufey et al. 2009). These numbers are very small compared to the accuracy of the determination of the obliquity, i.e. ≈ 5 arcsec.

6. Inverting the obliquity of Mercury

Recently, Margot et al. (2012) measured an obliquity of (2.04 ± 0.08) arcmin, and they used Peale's formula (Eq.1) to get $C/(mR^2) = 0.346 \pm 0.014$. In this work, we present alternative formulae that we propose to use to invert the obliquity of Margot et al. (2012). We can consider that we propose 4 new formulae. From an analytical (Eq.21) and a numerical studies (Eq.52, from Eq.38 & 39) we get 2 formulae. The influence of J_3, that we detect only numerically with the full equations of the system (Fig.4 & Eq.53) leads us to write down 2 new equations, in which the 2 obliquities given by the Eq.21 & 52 are corrected by $355.197 \times J_3$.

In considering that the spherical harmonics $C_{20} = -5.031 \times 10^{-5}$, $C_{22} = 8.088 \times 10^{-6}$, $C_{30} = 1.188 \times 10^{-5}$ and $C_{40} = 1.95 \times 10^{-5}$ are accurately known, we got the theoretical obliquity of Mercury 7 years after the date J2000.0 to be close to the mid-date of the radar observations. We considered that C was the only unknown parameter. In the analytical formula, we used the same dynamical parameters as Yseboodt & Margot (2006), i.e. $\iota = 8.6°$ and a regressional period of the ascending node set to 328 kyr. And we get

- Margot et al. (2012): $C/(mR^2) = 0.346 \pm 0.014$,

- Analytical formula (Eq.21): $C/(mR^2) = 0.34621 \pm 0.01358$,
- Numerical formula (Eq.52): $C/(mR^2) = 0.34576 \pm 0.01349$,
- Analytical formula (Eq.21) + J_3: $C/(mR^2) = 0.34550 \pm 0.01357$,
- Numerical formula (Eq.52) + J_3: $C/(mR^2) = 0.34506 \pm 0.01348$.

All our numbers are consistent with the ones coming from Peale's formula. The polar moment of inertia of Mercury could be $0.345mR^2$ instead of $0.346mR^2$, this difference is ridiculous with respect to the accuracy of the observations. Giving so many digits lacks of physical relevance, but is necessary to stress the tiny differences between our 4 formulae.

7. Conclusion

This study tackles the influence of usually neglected effects like the secular variations of the orbital elements, the tides and the higher order harmonics on the instantaneous obliquity of Mercury. The main goal is to invert it to get clues on the internal structure, in particular the polar inertial momentum C. Moreover, it gives optimized initial conditions of the orientation of the angular momentum of Mercury, at any time and for any values of the internal structure parameters, that can be directly used in numerical simulations. This is a refinement of (Noyelles & D'Hoedt 2012). These initial conditions have the advantage to be Laplace Plane free, they are instead based on the ecliptic, whose definition is robust. They have been obtained thanks to averaged equations of the rotational motion, suitable for long-term studies. We hope that they will help fitting the rotation of Mercury by future experiments, like the radioscience experiment in BepiColombo (Milani et al. 2001).

We have shown that the usually neglected effects have an influence smaller than 1 arcsec, while the observations have an accuracy of ≈ 5 arcsec. The determination of C can be at the most altered from $0.346mR^2$ to $0.345mR^2$, what does not fundamentally change our understanding of the internal structure of Mercury. The size of the molten core can be obtained from the longitudial librations of Mercury, but depends on whether we consider a rigid inner core or not (Van Hoolst et al. 2012).

Acknowledgements

This research used resources of the Interuniversity Scientific Computing Facility located at the University of Namur, Belgium, which is supported by the F.R.S.-FNRS under con-

vention No. 2.4617.07. It also benefited from the financial support of the contract Prodex C90253 “ROMEO” from BELSPO. Benoît Noyelles is F.R.S.-FNRS post-doctoral research fellow.

REFERENCES

Archinal B.A., A’Hearn M.F., Bowell E., Conrad A., Consolmagno G.J., Courtin R., Fukushima T., Hestroffer D., Hilton J.L., Krasinsky G.A., Neumann G., Oberst J., Seidelmann P.K., Stooke P., Tholen D.J., Thomas P.C. & Williams I.P., 2011, Report of the IAU Working Group on cartographic coordinates and Rotational Elements: 2009, CM&DA, 109, 101-135

Balogh A., Grard R., Solomon S.C., Schulz R., Langevin Y., Kasaba Y. & Fujimoto M., 2007, Missions to Mercury, Space Sci. Rev., 132, 611-645

Bertotti B. & Farinella P., 1990, Physics of the Earth and the Solar System, Kluwer

Bills B.G. & Comstock R.L., 2005, Forced obliquity variations of Mercury, J. Geophys. Res., 110, E04006

Bois E. & Rambaux N., 2007, On the oscillations in Mercury’s obliquity, Icarus, 192, 308-317

Colombo G., 1965, Rotational period of the planet Mercury, Nature, 208, 575

Cunningham, L.E., 1970, On the computation of the Spherical Harmonic Terms Needed during Numerical Integration of the Orbital Motion of an Artificial Satellite, Cel. Mech. 2, 207-216.

D’Hoedt S. & Lemaitre A., 2004, The spin-orbit resonant rotation of Mercury: a two degree of freedom Hamiltonian model, Cel. Mech. Dyn. Astr., 89, 267-283

D’Hoedt S. & Lemaitre A., 2008, Planetary long periodic terms in Mercury’s rotation: a two dimensional adiabatic approach, Cel. Mech. Dyn. Astr., 101, 127-139

D’Hoedt S., Noyelles B., Dufey J. & Lemaitre A., 2009, Determination of an instantaneous Laplace plane for Mercury’s rotation, Advances in Space Research, 44, 597-603

Dufey J., Noyelles B., Rambaux N. & Lemaitre A., 2009, Latitudinal librations of Mercury with a fluid core, Icarus, 203, 1-12

Hazewinkel M., 2001, Viète theorem, Encyclopedia of Mathematics, Springer

Laskar J., 1999, Introduction to frequency analysis, In: Proceedings of 3DHAM95 NATO Advanced Institute, vol.553, S'Agaro, pp. 134-150

Laskar J., 2005, Frequency Map Analysis and quasiperiodic decompositions, In:Benest et al. (Eds.), Hamiltonian Systems and Fourier Analysis: New Prospects for Gravitational Dynamics, Cambridge Sci. Publ., pp. 99-129

Margot J.-L., Peale S.J., Jurgens R.F., Slade M.A. & Holin I.V., 2007, Large longitude libration of Mercury reveals a molten core, Science, 316, 710-714

Margot J.-L., Peale S.J., Solomon S.C., Hauck II S.A., Ghigo F.D., Jurgens R.F., Yseboodt M., Giorgini J.D., Padovan S. & Campbell D.B., 2012, Mercury's moment of inertia from spin and gravity data, J. Geophys. Res., 117, E00L09

Milani A., Rossi A., Vokrouhlický D., Villani A. & Bonanno C., 2001, Gravity field and rotation state of Mercury from the BepiColombo Radio Science Experiments, Planet. Space Sci., 29, 1579-1596

Noyelles B., Dufey J. & Lemaitre A., 2010, Core-mantle interactions for Mercury, MNRAS, 407, 479-496

Noyelles B., Delsate N. & Carletti T., 2013, Equilibrium search algorithm of a perturbed quasi-integrable system, submitted, arXiv:1101.2138

Noyelles B. & D'Hoedt S., 2012, Modeling the obliquity of Mercury, Planet. Space Sci., 60, 274-286

Peale S.J., 1969, Generalized Cassini's laws, AJ, 74, 483-489

Peale S.J., 1976, Does Mercury have a molten core?, Nature, 262, 765-766

Peale S.J., 1981, Measurement accuracies required for the determination of a mercurian liquid core, Icarus, 48, 143-145

Peale S.J., Phillips R.J., Solomon S.C., Smith D.E. & Zuber M.T., 2002, A procedure for determining the nature of Mercury's core, Meteoritics and Planetary Science, 37, 1269-1283

Peale S.J., 2005, The free precession and libration of Mercury, Icarus, 178, 4-18

Peale S.J., 2006, The proximity of Mercury's spin to Cassini state 1 from adiabatic invariance, Icarus, 181, 338-347

Pettengill G.H. & Dyce R.B., 1965, A radar determination of the rotation of the planet Mercury, Nature, 206, 1240

Rappaport N.J., Iess L., Wahr J., Lunine J.I., Armstrong J.W., Asmar S.W., Tortora P., Di Benedetto M. & Racioppa P., 2008, Can Cassini detect a subsurface ocean in Titan from gravity measurements?, Icarus, 194, 711-720

Rambaux N. & Bois E., 2004, Theory of the Mercury's spin-orbit motion and analysis of its main librations, Astronomy and Astrophysics, 413, 381-393

Smith D.E., Zuber M.T., Phillips R.J, Solomon S.C., Hauck II S.A., Lemoine F.G., Mazarico E., Neumann G.A., Peale S.J., Margot J.-L., Johnson C.L., Torrence M.H., Perry M.E., Rowlands D.D., Goossens S., Head J.W. & Taylor A.H., 2012, Gravity field and internal structure of Mercury from MESSENGER, Science, 336, 214-217

Standish E.M., 1998, JPL planetary and lunar ephemeris, DE405/LE405. JPL Interoffice Memorandum IOM 312.D-98-048

Van Hoolst T., Rambaux N., Karatekin Ö., Dehant V. & Rivoldini A., 2008, The librations, shape, and icy shell of Europa, Icarus, 195, 386-399

Van Hoolst T., Rivoldini A., Baland R.-M. & Yseboodt M., 2012, The effect of tides and an inner core on the forced longitudinal libration of Mercury, Earth and Planetary Science Letters, 333-334, 83-90

Veasey M. & Dumberry M., 2011, The influence of Mercury's inner core on its physical libration, Icarus, 214, 265-274

Yseboodt M. & Margot J.-L., 2006, Evolution of Mercury's obliquity, Icarus, 181, 327-337

Appendix A

We collect the various coefficients of the form $[j]_{nm}$, with $j, n, m \in \mathbb{N}$, from Section 2.4. If we introduce the notation $c_x = \cos(x)$, $s_x = \sin(x)$ they can be written in the form:

At second order in $\langle V_{20} \rangle$:

$$[1]_{20} = 3\,(1 + 3c_{2i})\,c_{2K}\ ,\ [2]_{20} = 48 c_i c_K s_i s_K\ ,\ [3]_{20} = -6 c_{2K} s_i^2\ .$$

At second order in $\langle V_{22}\rangle$:

$$[1]_{22} = 48c_{i/2}^4c_{K/2}^4 \ , \ [2]_{22} = 12\left(1+c_i\right)\left(1+c_K\right)s_is_K \ , \ [3]_{22} = 18s_i^2s_K^2 \ ,$$
$$[4]_{22} = 48s_{i/2}^2s_is_{K/2}^2s_K \ , \ [5]_{22} = 48s_{i/2}^4s_{K/2}^4 \ ,$$

in $\langle v_{20}\rangle$ and

$$[6]_{22} = -4c_{K/2}^4s_i^2 \ , \ [7]_{22} = 4\left(1+c_K\right)s_ic_is_K \ , \ [8]_{22} = -\left(1+3c_{2i}\right)s_K^2 \ ,$$
$$[9]_{22} = 4c_i\left(c_K-1\right)s_is_K \ , \ [10]_{22} = -4s_i^2s_{K/2}^4$$

in $\langle u_{20}\rangle$. At order three we have in $\langle V_{30}\rangle$:

$$[1]_{30} = -30s_{i/2}^2s_i^2s_K^3 \ , \ [2]_{30} = 30\left(c_i-1\right)\left(1+3c_i\right)c_Ks_is_K^2 \ ,$$
$$[3]_{30} = -\frac{3}{2}\left(13+20c_i+15c_{2i}\right)\left(3+5c_{2K}\right)s_{i/2}^2s_K \ ,$$
$$[4]_{30} = -\frac{3}{4}\left(3c_K+5c_{3K}\right)\left(s_i+5s_{3i}\right) \ , \ [5]_{30} = \frac{3}{4}c_{i/2}^2\left(13-20c_i+15c_{2i}\right)\left(s_K+5s_{3K}\right) \ ,$$
$$[6]_{30} = 30\left(1+c_i\right)\left(3c_i-1\right)c_Ks_is_K^2 \ , \ [7]_{30} = -15\left(c_i-1\right)\left(1+c_i\right)^2s_K^3 \ .$$

The fourth order coefficients, beeing part of $\langle v_{40}\rangle$, turn out to be:

$$[1]_{40} = \frac{3}{64}\left(9+20c_{2i}+35c_{4i}\right)\left(9+20c_{2K}+35c_{4K}\right) \ , \ [2]_{40} = \frac{15}{8}\left(2s_{2i}+7s_{4i}\right)\left(2s_{2K}+7s_{4K}\right) \ ,$$
$$[3]_{40} = 15\left(5+7c_{2i}\right)\left(5+7c_{2K}\right)s_i^2s_K^2 \ , \ [4]_{40} = 840c_ic_Ks_i^3s_K^3 \ , \ [5]_{40} = 105s_i^4s_K^4 \ .$$

The fourth order coefficients in $\langle u_{40}\rangle$ are:

$$[6]_{40} = \frac{15}{4}\left(5+7c_{2i}\right)\left(9+20c_{2K}+35c_{4K}\right)s_i^2 \ , \ [7]_{40} = 840s_{\frac{i}{2}}^4s_i^2s_K^4 \ ,$$
$$[8]_{40} = 6720\left(2c_{i/2}+c_{3i/2}\right)c_Ks_{i/2}^5s_K^3 \ ,$$
$$[9]_{40} = 120\left(9+14c_i+7c_{2i}\right)\left(5+7c_{2K}\right)s_{i/2}^4s_K^2 \ ,$$
$$[10]_{40} = 30\left(19c_{i/2}+7\left(2c_{3i/2}+c_{5i/2}\right)\right)s_{i/2}^3\left(2s_{2K}+7s_{4K}\right) \ ,$$
$$[11]_{40} = -30c_{i/2}^3\left(19s_{i/2}+7\left(s_{5i/2}-2s_{3i/2}\right)\right)\left(2s_{2K}+7s_{4K}\right) \ ,$$
$$[12]_{40} = 120c_{i/2}^4\left(9-14c_i+7c_{2i}\right)\left(5+7c_{2K}\right)s_K^2 \ ,$$
$$[13]_{40} = 6720c_{i/2}^5c_K\left(s_{3i/2}-2s_{i/2}\right)s_K^3 \ , \ [14]_{40} = -210\left(c_i-1\right)\left(1+c_i\right)^3s_K^4 \ .$$

Table 4: Coefficients involved in the Eq.40 to 43.

N	α	β	γ	δ
1	-9.6916394157	-1.022791×10^{7}	1.224118×10^{7}	-0.041284174514
2	57.319667133	-1.495053×10^{8}	1.8067315×10^{8}	-15.290923597
3	-288.588048	-6.75794×10^{8}	8.648745×10^{8}	–
4	109.5839605	-2.3327045×10^{9}	-2.8315945×10^{9}	–
5	9618.2490875	-5.967955×10^{9}	$-1.4620515 \times 10^{10}$	-4270.5575456
6	5690.3083952	-3.29021×10^{9}	4.59872×10^{9}	-5791.2841683
7	160882.75	-1.563842×10^{10}	–	–
8	-330146.25	$-3.3956545 \times 10^{10}$	–	–
9	-307545.35	-3.441592×10^{10}	–	–
10	-879441.5	-4.59746×10^{10}	–	–
11	-1025209.5	-5.12722×10^{10}	–	–
12	760424	-7.318535×10^{10}	–	–
13	-3583265	$-1.7097535 \times 10^{11}$	–	–
14	-1352596	-1.522164×10^{11}	–	–
15	-1475953.5	-1.554497×10^{11}	–	–
16	-4788455	$-2.4530905 \times 10^{11}$	–	–
17	0.0459703076	-111936.3	133840.35	0.00068014043987
18	0.5097512707	-474698	568708	-0.0063487867442
19	3.6758306831	-2005542	2431534	-0.32882074509
20	20.470309592	-12322835	-31382330	1.6246447377
21	22.351343806	-8470000	10602865	-4.3502813922
22	1.8968370715	-25710160	-28807205	-14.991580755
23	28.007891612	-25704595	-30518425	0.75276141087
24	151.69560968	-52410050	-127924300	-54.254151937
25	11.320467298	-35729050	384.87733645	–
26	60.949766585	-91723450	-262171000	275.67522095
27	93.149257619	-96422550	-265414800	257.09346578
28	256.01109782	-108893750	-1098.8078842	–
29	93.896968203	-109386550	-1017.8654389	–
30	880.39601125	-223772150	-4722.8636039	–
31	-390.02956574	-145710250	2105.3653480	–
32	1929.3930214	-404092500	-8327.8625575	–
33	2613.8902647	-456302000	-4855.3715926	–
34	-2905.1715	-438245500	–	–

Table 5: Relative influence on the mean obliquity of usually neglected effects. The amplitude of the free librations can be seen as an estimation of the error due to theory.

Effect	Influence on obliquity
Free librations	< 750 mas
C_{30}	≈ 250 mas
Tides	≈ 100 mas
Polar motion	≈ 80 mas (Noyelles et al. 2010)
Short-period librations	< 20 mas (Dufey et al. 2009)
Secular drift	≈ 10 mas over 20 years
C_{40}	negligible